How to cite: *Angew. Chem. Int. Ed.* **2023**, *62*, e202310445
doi.org/10.1002/anie.202310445

Strained Molecules

Forcing Twisted 1,7-Dibromoperylene Diimides to Flatten in the Solid State: What a Difference an Atom Makes

*Konstantis F. Konidaris, Marco Zambra, Francesco Giannici, Antonietta Guagliardi, and Norberto Masciocchi**

Abstract: Perylene diimides (PDI) are workhorses in the field of organic electronics, owing to their appealing n-semiconducting properties. Optimization of their performances is widely pursued by bay-atom substitution and diverse imide functionalization. Bulk solids and thin-films of these species crystallize in a variety of stacking configurations, depending on the geometry of the stable conformation of the polyaromatic core. We here demonstrate that 1,7-dibromo-substituted perylene diimides, PDI(H_2Br_2), possessing a heavily twisted conformation in the gas phase, in solution and in the solids, can be easily flattened in the solid state into centrosymmetric molecules if the polyaromatic cores form π–π stabilized chains. This is achieved by using axial residues with low stereochemical hindrance, as guaranteed by a single CH_2/NH spacer directly linked to the imide function. Structural powder diffraction and DFT calculations on four newly designed species of the PDI(H_2Br_2) class coherently show that, thanks to the flexibility of the N–X–Ar link (X=CH_2/NH), flat cores are indeed obtained by overcoming the interconversion barrier between twisted atropoisomers, of only 26.5 kJ mol^{-1}. This strategy may then be useful to induce "anomalously flat" polyaromatic cores of different kinds (substituted acenes/rylenes) in the solid state, towards suitable crystal packing and orbital interactions for improved electronic performances.

In the last decades, naphthalene- (NDI) and perylene- (PDI) diimides have raised the interest of many researchers, in academia and industry, as promising materials for a number of applications, namely as organic semiconductors, photo-degradation catalysts, ion and organic pollutant sensors, pigments, to mention a few.[1] Among *n*-type organic semiconductors, PDIs have become highly promising substitutes to fullerene-based materials, thanks to their chemical and thermal robustness, ease of functionalization, high electron-accepting ability and electron mobility, which are all valuable features in developing new organic (opto)electronic devices.[2] Some of the best performers in this field possess cyano residues in the 1,7-bay positions of the perylene core. CN groups are indeed known to increase the materials electron affinity (EA) up to ca. 4.3 eV, while simultaneously maintaining a flat (and centrosymmetric) geometry, favouring (in the solid state) the formation of an extended stack of π–π interacting molecules.[3] Larger EA values (e.g., 4.82 eV) are also obtained, but these poly-CN bay-substituted derivatives are found to be extremely unstable.[4]

The introduction of CN groups is normally obtained through the intermediacy of the core-substituted Br derivatives (see Scheme 1), followed by the nucleophilic substitutions promoted by reaction with CuCN.[5] 1,7-dibromoperylene intermediates [briefly, PDI(H_2Br_2)] have been the subject of more limited investigations, also because the

[*] Dr. K. F. Konidaris, M. Zambra, Prof. N. Masciocchi
Dipartimento di Scienza e Alta Tecnologia and To.Sca.Lab
University of Insubria
via Valleggio 11, 22100 Como (Italy)
E-mail: norberto.masciocchi@uninsubria.it
Prof. F. Giannici
Dipartimento di Fisica e Chimica "Emilio Segrè"
Università di Palermo
viale delle Scienze, Ed.17, 90128 Palermo (Italy)
Dr. A. Guagliardi
Institute of Crystallography and To.Sca.Lab
C.N.R., National Research Council
via Valleggio 11, 22100 Como (Italy)

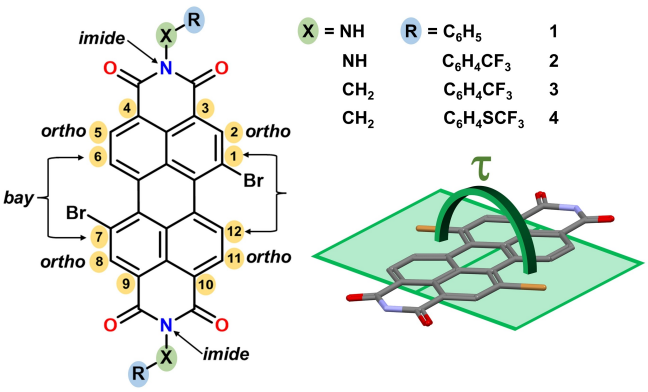

Scheme 1. Left: connectivity and labelling of 1,7, dibromoperylene diimides. Right: the geometric definition of torsion angle τ. For simplicity, the δ values discussed in the following are δ = 180-τ.

heavily twisted nature of the perylene core (measured, e.g., by δ, the deviation from 180° of the Br···C···C···Br torsion angle τ illustrated in Scheme 1) somewhat contrasts the tendency of these molecules to pack, in a solid, into "electronically" efficient π–π stacks.

In this regard, a recent report demonstrated that molecular "contortion", *per se*, is not a detrimental factor toward high-performance materials.[6] However, besides this notable exception, the paucity of other pertinent crystal structures present in the literature does not permit to work on a statistically rich set of PDI(H_2Br_2) derivatives for assessing the role of core twisting on the charge transport properties, and the flat core apparently remains a strict requirement. Indeed, there is a general consensus that higher charge mobilities are associated with small-molecule core planarity and, therefore, with a more effective π–π overlap. This is valid not only for PDI-based systems, but also for oligothiophenes, fluorenes and acenes.[7] On the structural side, the available stereochemical data (collected in Table 1) include a surprising (and trustworthy) outlier[8] (CSD Code: WUFKIT), for which the origin of the "anomalous" (flat) molecular conformation is not discussed. Herein, we investigate four new PDI species (**1**–**4**) that systematically show the same structural feature, and unveil its driving force. Following a molecular design approach, we have employed axial imide substituents with low stereochemical hindrance (CH_2–R or NH–R) to promote the formation of stacked "core-flattened" PDI molecules. Our analysis is supported by experimental powder diffraction evidence and by DFT calculations, highlighting the energetics of flattening and of the atropoisomeric interconversion.

As already reported in the literature, many of these systems are rather insoluble in common organic solvents. Accordingly, they cannot be easily recrystallized from solution or, often, give poorly diffracting single crystals, in the form of extremely thin needles. This leaves, in the structural chemists' hands, only the possibility to actively use X-ray powder diffraction (XRPD) methods. Though relying on reduced atomic resolution data (bond lengths and angles of moderately complex molecular solids need to be heavily constrained), *structural* XRPD has become an important substitute for partially rigid structure determinations and has been fruitfully used to reliably determine location, orientation and packing features of several organics (polymorphic drugs, covalent organic frameworks, organic semiconductors, etc.).[16]

Our recent studies on poly-fluorinated alkyl- and aryl-imides and hydrazimides based on the smaller NDI congeners demonstrated the viability of this structural method, and showed that π–π stacking features of planar aromatic cores can be successfully determined by XRPD structural analysis also in the absence of single-crystal specimens of suitable size and quality.[17] On shifting our interest toward larger aromatic cores, where higher EAs are obtained and, if suitably arranged in the solid, electron mobility is also enhanced, we prepared several 1,7-dibromo-PDI derivatives of the (H_2Br_2) type, all of them showing highly crystalline powder patterns. The four isolated species (numbered according to the labels shown in Scheme 1) were synthesized at room temperature (RT) according to a modified literature procedure.[18] Details of the synthesis, characterization and XRPD structural analysis are reported in the SI.

Surprisingly, symmetry and density constraints, jointly with the complete knowledge of molecular connectivity, ended up with structural models for species **1**–**4** with *all* molecules possessing crystallographically imposed C_i symmetry, that is containing planar PDI cores (Figures 1b, S16 and S17). The exploration of twisted conformations (ordered, in *Cc*, and disordered, in *C2/c* space groups) was also tested by progressively changing the δ value in the ±35° range, but all statistical indicators (R_{wp}, R_p and R_{Bragg} agreement factors, see Figure 1a) indicated PDI core planarity. Note that the disordered model in space group *C2/c* addresses the possible presence of a 50:50 mixture of two chiral (twisted) atropoisomers (M and P), in random or

Table 1: Synoptic collection of geometrical properties of axially imide-substituted 1,7-dibromo PDIs (solid phases). Type II stands for a N–X substitution with a secondary X atom (X = C, N, **in bold**), whereas Type III and Ar refer to a tertiary and arylic X atom, respectively.

CSD Code	Imide substituent	δ [°]	Type	Color	Ref.
ADUCUA	*Bulky* siloxane	25.7	II	orange	[9]
JAJWAT	Cyclohexyl	32.0, 33.5	III	red	[10]
JAPXII	2,6-di*iso*propylphenyl	22.8	Ar	orange	[11]
NIMCOD	Cyclohexyl	25.6	III	orange	[12]
SIJYUG	Ethylpropyl	29.7	III	orange	[13]
VEBXEJ	Phenylethyl	22.5	III	red	[14]
WUFKIT	Propylacetate	0.0	II	red	[8]
1, 2280624[15]	Phenyl-**N**H-	0.0	II	red	This work
2, 2280625	4-CF_3-phenyl-**N**H-	0.0	II	red	This work
3, 2280626	4-CF_3-phenyl-**C**H_2-	0.0	II	red	This work
4, 2280623	4-SCF_3-phenyl-**C**H_2-	0.0	II	red	This work

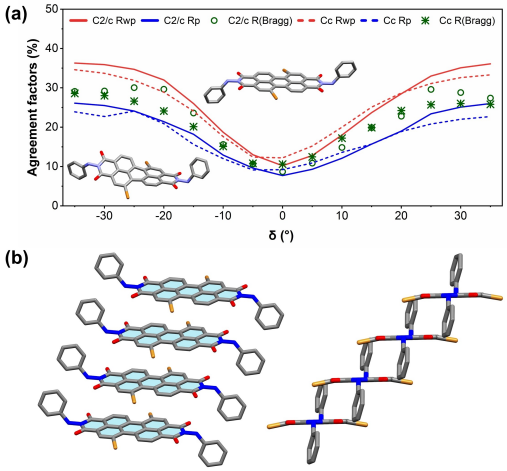

Figure 1. a) Variations of R_{wp}, R_p and R_{Bragg} agreement factors upon inserting an ordered twisted model in sg *Cc*, or 50:50 disordered about the inversion center in sg *C2/c*. Clear minima are found for δ ≈ 0°. The insets show the DFT-optimized geometry for gas-phase molecule **1**, with δ ≈ 32° (bottom left) and the flat conformation found in the solid (top center). b) The π–π stacked molecules present in **1**, viewed in two different projections, demonstrating that the extra atom (here, the N_{Ar} one, in blue) enables the bending of the Ar residue, limiting steric encumbering. Similar considerations apply to compounds **2**–**4**.

even in "column-segregated" disposition, both models being easily dismissed by the sharp minima of the statistical R-factors indicators, shown in Figure 1a (red and blue solid lines).

These repeated observations are, however, in stark contrast with the expected dihedral angles (δ) observed in most congeners (Table 1) and also in other bay-substituted pyrenes,[19] and with computational predictions of the stability and geometry of these systems. Indeed, energetic minima with twisted conformations of two chiral atropoisomers (M and P), with δ values falling in the 25–35° range,[20] are expected. Nearly identical δ values of ca. 32.0° (±0.2°) were calculated for compounds **1**–**4** using a range-separated hybrid functional (CAM-B3LYP), and even for Hartree-Fock optimizations (regardless of the basis set), confirming that such torsion in an isolated molecule does not depend on the level of theory used. For a simplified version of compound **1**, obtained by eliminating the pendant hydrazimido arms (defined as compound $\mathbf{0_{Br}}$ in Table S3), the conformational space was studied at a higher level of theory (B3LYP/cc-pVTZ), identifying an optimized transition state with C_{2h} symmetry (Figure 2). This conformation ideally lies midway across the M→P interconversion pathway from one atropoisomer to the other, at δ = 0°, with a rather low $\Delta E^{\ddagger}$ value of only 26.5 kJ mol^{-1} (very much in line with 25.1 kJ mol^{-1}, a value quoted for the core twist barrier in 1,7-dibrominated PDIs[13]). A more extended study of racemization barriers of perylene diimides mentions, for H_2Br_2 substitution, a $\Delta G^{\ddagger}$ value of ca. 40 kJ mol^{-1}, a value low enough to make HPLC enantiomeric separation impossible at RT[20] because of a rapid interconversion rate. The transition state at δ = 0°, however, is a maximum in the interconversion pathway in the gas-phase (Figure 2) and has nearly null lifetime (in the *ps* regime, compatible with molecular vibrations). Therefore, the stabilization of *flat* PDI(H_2Br_2) cores needs to hang on different effects. As an additional test, energy minimization for a slightly distorted centrosymmetric molecule located a shallow minimum (ca. 6 kJ mol^{-1} below the transition state), where a planar PDI core is associated with Br atoms slightly off the poly-aromatic plane.

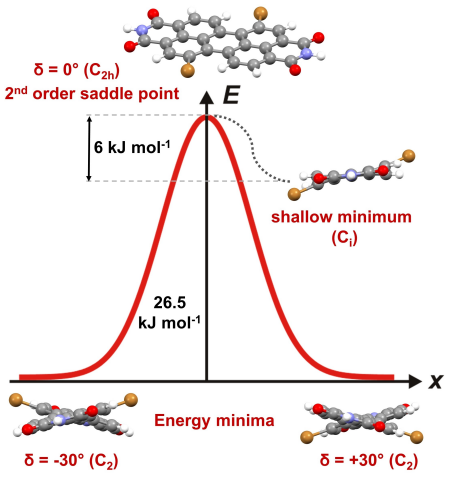

Figure 2. DFT-calculated energy profile for the P→M atropoisomeric interconversion of compound $\mathbf{0_{Br}}$ in the gas phase, indicating that the geometry of the transition state at δ = 0° is only 26.5 kJ mol^{-1} above the minimum, and can be stabilized, in the solid, by the presence of strong(er) intermolecular interactions. The presence of a local minimum, ca. 6 kJ mol^{-1} below the flat transition state, is also shown (B3LYP/cc-pVTZ level). The Kohn–Sham energies and shapes of the frontier orbitals are collected in the Supporting Information and nicely demonstrate that they are only marginally affected by twisting, with less than 2% relative energy changes and occasional cross-over for the HOMO-1/HOMO-2 and HOMO-3/HOMO-4 orbitals. Additionally, also the ring aromaticity is not substantially changed, with the central ring maintaining a substantial "non-aromatic" character (see Table S6).

Worthy of note, ^{1}H NMR signals of the two benzylic protons (equivalent in the free amine and in the *p*-CF_3- and *p*-SCF_3-benzylamine of the NDI type,[21] but ideally distinct and diastereotopic in compounds **3** and **4**), provide further insights on the M, P atropoisomer conversion rate. For **3** and **4**, a doublet of doublets is expected to appear side by side with very similar chemical shifts, being the origin of molecular chirality distant enough. However, if the geminal $^2J_{H\text{-}H}$ coupling constant is similar to Δν (the difference of resonance frequencies of the two distinct protons), then the two central peaks may merge and an anomalous triplet is observed (Figure S10), with the most intense peak enhanced by the well-known roofing effect. The presence of this triplet also gives an estimate of the interconversion rate, which, at RT, is slower than the NMR timescale (taken for simplicity as 10^{-8} s). Therefrom, an upper limit of the interconversion kinetic constant *k* may be calculated, corresponding to an approximate $\Delta G^{\ddagger}$ value of 28 kJ mol^{-1} (from Eyring's equation), in line with our DFT calculations. We also note that the colours of these solids are practically identical, in line with the *solution* UV/Vis absorbance spectra, which change very little on passing from one species to the other (Table S1). Indeed, a characteristic triplet (attributed to the S_0–S_1 vibronic sequence[22]), covering the entire 450–550 nm range and peaking near 530 nm, is constantly observed and is only marginally affected by the bromination level and, hence, by the progressively increased twist.[8] This can be explained by the fact that frontier orbitals mostly reside on the poly-aromatic core, forcing the predicted transition frequencies to remain remarkably unaffected by substitutions in the imide position, whereas minor shifts (<7 nm) have been measured in differently brominated species.[8]

The twisted-core conformation is a constant feature in all predicted gas-phase geometries. Twisted cores are also maintained in the solid state as well, for systems bearing bulky enough imide residues (as if they were only marginally affected by the crystal-packing environment). Indeed, for all the species with branched alkyls/aryls and tertiary C atoms (labelled as III in Table 1), the close approach of PDI cores of distinct molecules is very difficult. Only the bis-propylacetate 1,7-dibromo-substituted PDI molecule, which bears a stretched aliphatic residue in the imide position (type II in Table 1), is flat. Consequently, it shows the presence, in the solid, of (ideally infinite) ladders of π–π stacked moieties, characterized by the χ, ψ and *d* parameters[17b] (sketched in the inset of Figure 3 and Figure S19) of 79.5°, 48.6° and 3.51 Å, respectively (Table S2). When plotted in the χ, ψ plane, these values (in blue) manifest packing features very similar to those determined for **1**–**4** (black markers). Additional points (red markers) are also drawn for flat NDI cores

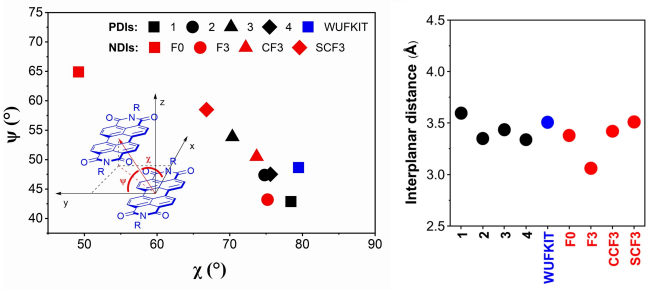

Figure 3. Left: positioning in χ, ψ plane of the stacking parameters of the flat PDI(H_2Br_2) moieties listed in Table 1 (black/blue markers), jointly with the values for analogous NDIs with identical imide residuals (red markers); the inset sketches the geometrical meaning of the χ, ψ descriptors. Right: the interplanar distances (*d*) of parallel PDI/NDI cores. The pertinent values are gathered in Table S2.

with analogous imide derivatization as in **1**–**4**, which show a slightly higher structural versatility.[17d]

The appealing hypothesis that the occurrence, in the solid state, of (necessarily strained) flat PDI(H_2Br_2) cores must be attributed to stabilizing intramolecular interactions, therefore, finds a very good confirmation whenever the axial imides have limited steric encumbrance. Indeed, thanks to additional flexibility provided by the NH/CH_2 spacers in the hydrazido/benzyl links present in **1**–**4** (but not in the *tertiary* alkyls or aryls of the twisted molecules—Table 1), bending of the aryl substituents (off the average poly-aromatic molecular plane) occurs. That steric effects do indeed influence the nature and extent of π–π stacking was already recognized, with a special focus on core-unsubstituted PDIs (ideally flat *also* in the gas phase).[23]

An alternative interpretation for PDI core flattening can be however put forward: "axial" aromatic residues may act as paddles, where additional packing forces arise, overcoming the M→P interconversion barrier. However, as flattening in the solid state occurs also for a swinging, non-rigid, residue (the propylacetate in WUFKIT), this effect, if present, must be of second order. These observations thus confirm that the flexibility induced by the NH/CH_2 spacers is substantially independent of the aliphatic/aromatic nature of the (hydraz)imide.

Worthy of note, the occurrence of infinite stacks of homochiral (twisted) molecules, where the offset of the Br atoms generates a weak dipole (0.35 D in $\mathbf{0_{Br}}$) may further stabilize, through an infinite number of dipolar interactions, the twisted conformer. However, using Ciftja's model[24] and the stacking parameters shown in Figure 3, such stabilization falls near 0.1 kJ mol^{-1}, that is two orders of magnitude lower than π–π stacking, and is, in our discussion, a negligible term.

Compounds **1**–**4** stack according to the *tight-long-y* description proposed by Maini and co-workers,[25] characterized by parallel molecules piled with a larger shift in the *y* direction than along the molecular axis, taken as *x*. Though not rare, only 17 out of 142 PDI-based objects retrieved in the CSD crystallize in this class.[25] Recent papers have reported on the stabilizing effect of intermolecular contacts in PDI oligomers, estimated to lie in the 65–85 kJ mol^{-1} regime per dimeric contact.[26] Following Vura-Veis et al. model,[27] species **2**–**4**, which possess similar long- and short-axis shifts (in the 1.2–1.6 Å and 2.8–3.3 Å ranges, respectively), fall far away from the highly attractive basin characterized by 75 (and higher) kJ mol^{-1} binding energy value (species **1** appears slightly different in that a larger short-axis shift, 4.0 Å, is present, falling in a region not investigated in the theoretical study of ref. [27]). However, the wide and slightly corrugated shape of the binding energy surface makes these species still belong to an attractive configuration characterized by a non-negligible binding energy of ca. 60 kJ mol^{-1}. This value is twice stronger than that of the perylene dimer and is attributed to electrostatic π-hole···C=O interactions between the carbonyl of one monomer with the electron deficient π-rings of the other.[26] Consequently, if this value overcomes the energy loss due to core flattening, then, in the solids, infinite ladders running across the crystals with a short translation vector are expected, and indeed observed (Figure 1b and Figure S18), for PDI cores not at all willing to be flat in the gas and (dilute) solution phases.

We have thus demonstrated that, in the case of 1,7-bay substitution, the molecular packing is the result of the competition between the non-covalent interactions due to the bromine substituents (towards a twisted conformer) and the formation of stacks of parallel perylene cores (favoured by planarity). So, while introducing suitable substituents in the core may be advantageous for regulating HOMO and LUMO energies, only the use of "sterically innocent" imide residues makes it possible to obtain suitably tuned stacking interactions apt to ideally promote efficient charge transport.[28]

Supporting Information

The Supporting Information file contains details on the synthesis and spectroscopic characterization, on the structural powder diffraction analysis and on DFT calculations. The authors have cited additional references within the Supporting Information.[29–34]

Acknowledgements

We acknowledge financial support by the Italian MUR (Project PRIN 2017L8WW48). We also thank F. Ferrante (University of Palermo) for fruitful discussions. Conceptualization: K.F.K. and N.M.; Investigation and Methodology: M.Z., K.F.K. and F.G; Funding Acquisition: F.G., A.G. and N.M.; Writing—original draft: K.F.K. and N.M.; Writing—review and editing: F.G. and A.G.

Conflict of Interest

The authors declare no conflict of interest.

Data Availability Statement

The data that support the findings of this study are available in the supplementary material of this article.

Keywords: perylene diimides · stereochemistry · π–π stacking · core substitution · powder diffraction

[1] a) X. Zhan, A. Facchetti, S. Barlow, T. J. Marks, M. A. Ratner, M. R. Wasielewski, S. R. Marder, *Adv. Mater.* **2011**, *23*, 268–284; b) J. Cao, S. Yang, *RSC Adv.* **2022**, *12*, 6966–6973; c) Y. Li, X.-L. Zhang, D. Liu, *J. Photochem. Photobiol. C* **2021**, *48*, 100436; d) W. Zhou, G. Liu, B. Yang, Q. Ji, W. Xiang, H. He, Z. Xu, C. Qi, S. Li, S. Yang, C. Xu, *Sci. Total Environ.* **2021**, *780*, 146483; e) O. Krupka, P. Hudhomme, *Int. J. Mol. Sci.* **2023**, *24*, 6308.

[2] a) A. Nowal-Król, K. Shoyama, M. Stolte, F. Würthner, *Chem. Commun.* **2018**, *54*, 13763–13772; b) Q. He, P. Kafourou, X. Hu, M. Heeney, *SN Appl. Sci.* **2022**, *4*, 247.

[3] a) B. A. Jones, M. J. Ahrens, M.-H. Yoon, A. Facchetti, T. J. Marks, M. R. Wasielewski, *Angew. Chem. Int. Ed.* **2004**, *43*, 5353–6366; b) J. Gao, C. Xiao, W. Jiang, Z. Wang, *Org. Lett.* **2014**, *16*, 394–397; c) M. Barra, F. Chiarella, F. Chianese, R. Vaglio, A. Cassinese, *Electronics* **2019**, *8*, 249.

[4] Q. Ye, J. Chang, K.-W. Huang, X. Shi, J. Wu, C. Chi, *Org. Lett.* **2013**, *15*, 1194–1197.

[5] a) L. R. Subramanian, *Sci. Synth.* **2004**, *19*, 173–195; b) J. Chang, Q. Ye, K.-W. Huang, J. Zhang, Z.-K. Chen, J. Wu, C. Chi, *Org. Lett.* **2012**, *14*, 2964–2967.

[6] C. Schaak, A. M. Evans, F. Ng, M. L. Steigerwald, C. Nuckolls, *J. Am. Chem. Soc.* **2022**, *144*, 42–51.

[7] H. Usta, A. Facchetti, in *Large Area and Flexible Eletronics* (Eds.: M. Caironi, Y.-Y. Noh), Wiley-VCH, Weinheim, Ch. 1, pp. 1–100.

[8] K. Nagarajan, A. R. Mallia, V. Sivaranjana Reddy, M. Hariharan, *J. Phys. Chem. C* **2016**, *120*, 8443–8450.

[9] Y. Shao, X. Zhang, K. Liang, J. Wang, Y. Lin, S. Yang, W.-B. Zhang, M. Zhu, B. Sun, *RSC Adv.* **2017**, *7*, 16155–16162.

[10] F. Würthner, V. Stepanenko, Z. Chen, C. R. Saha-Moller, N. Kocher, D. Stalke, *J. Org. Chem.* **2004**, *69*, 7933–7939.

[11] C.-C. Chao, M.-K. Leung, Y. O. Su, K.-Y. Chiu, T.-H. Lin, S.-J. Shieh, S.-C. Lin, *J. Org. Chem.* **2005**, *70*, 4323–4331.

[12] B. A. Llewellyn, A. G. Slater, G. Goretzki, T. L. Easun, X.-Z. Sun, E. Stephen Davies, S. P. Argent, W. Lewis, A. Beeby, M. W. George, N. R. Champness, *Dalton Trans.* **2014**, *43*, 85–94.

[13] P. Rajasingh, R. Cohen, E. Shirman, L. J. W. Shimon, B. Rybtchinski, *J. Org. Chem.* **2007**, *72*, 5973–5979.

[14] X. Shang, J. Ahn, J. H. Lee, J. C. Kim, H. Ohtsu, W. Choi, I. Song, S. K. Kwak, J. H. Oh, *ACS Appl. Mater. Interfaces* **2021**, *13*, 12278–12285.

[15] Deposition numbers 2280624 (for **1**), 2280625 (for **2**), 2280626 (for **3**), and 2280623 (for **4**) contain the supplementary crystallographic data for this paper. These data are provided free of charge by the joint Cambridge Crystallographic Data Centre and Fachinformationszentrum Karlsruhe Access Structures service.

[16] a) R. Černý, *Crystals* **2017**, *7*, 142; b) J. A. Kaduk, S. J. L. Billinge, R. E. Dinnebier, N. Henderson, I. Madsen, R. Černý, M. Leoni, L. Lutterotti, S. Thakral, D. Chateigner, *Nat. Rev. Methods Primer* **2021**, *1*, 77.

[17] a) L. Ferlauto, F. Liscio, E. Orgiu, N. Masciocchi, A. Guagliardi, F. Biscarini, P. Samorì, S. Milita, *Adv. Funct. Mater.* **2014**, *24*, 5503–5510; b) S. Milita, F. Liscio, L. Cowen, M. Cavallini, B. A. Drain, T. Degousée, S. Luong, O. Fenwick, A. Guagliardi, B. C. Schroeder, N. Masciocchi, *J. Mater. Chem. C* **2020**, *8*, 3097–3112; c) V. M. Abbinante, G. García-Espejo, G. Calabrese, S. Milita, L. Barba, D. Marini, C. Pipitone, F. Giannici, A. Guagliardi, N. Masciocchi, *J. Mater. Chem. C* **2021**, *9*, 10875–10888; d) V. M. Abbinante, M. Zambra, G. García-Espejo, C. Pipitone, F. Giannici, S. Milita, A. Guagliardi, N. Masciocchi, *Chem. Eur. J.* **2023**, *29*, e202203441.

[18] R. T. Weitz, K. Amsharov, U. Zschieschang, E. B. Villas, D. K. Goswami, M. Burghard, H. Dosch, M. Jansen, K. Kern, H. Klauk, *J. Am. Chem. Soc.* **2008**, *130*, 4637–4645.

[19] X. Yang, F. Rominger, M. Mastalerz, *Org. Lett.* **2018**, *20*, 7270–7273.

[20] P. Osswald, F. Würthner, *J. Am. Chem. Soc.* **2007**, *129*, 14319–14326.

[21] a) M. R. Ajayakumar, P. Mukhopadhyay, S. Yadav, S. Ghosh, *Org. Lett.* **2010**, *12*, 2646–2649; b) L. Zhao, D. Zhang, Y. Zhu, S. Peng, H. Meng, W. Huanga, *J. Mater. Chem. C* **2017**, *5*, 848–853.

[22] M. Oltean, A. Calborean, G. Mile, M. Vidrighin, M. Iosin, L. Leopold, D. Maniu, N. Leopold, V. Chiş, *Spectrochim. Acta Part A* **2012**, *97*, 703–710.

[23] R. S. Wilson-Kovacs, X. Fang, M. J. L. Hagemann, H. E. Symons, C. F. J. Faul, *Chem. Eur. J.* **2022**, *28*, e202103443.

[24] O. Ciftja, *Res. Phys.* **2020**, *17*, 103178.

[25] F. Marin, A. Zappi, D. Melucci, L. Maini, *Mol. Syst. Des. Eng.* **2023**, *8*, 500–515.

[26] a) Y. Geng, H.-B. Li, S, -X. Wu, Z.-M. Su, *J. Mater. Chem.* **2012**, *22*, 20840–20851; b) S. Parida, S. K. Patra, S. Mishra, *ChemPhysChem* **2022**, *23*, e202200361.

[27] J. Vura-Weis, M. A. Ratner, M. R. Wasielewski, *J. Am. Chem. Soc.* **2010**, *132*, 1738–1739.

[28] M. C. Ruiz Delgado, E.-G. Kim, D.A Da Silva Filho, J.-L. Brédas, *J. Am. Chem. Soc.* **2010**, *132*, 3375–3387.

[29] TOPAS–R, V. 3.0, **2005**, Bruker AXS, Karlsruhe, Germany.

[30] A. A. Coelho, *J. Appl. Crystallogr.* **2003**, *36*, 86–95.

[31] Gaussian 16, Revision C.01, M. J. Frisch, G. W. Trucks, H. B. Schlegel, G. E. Scuseria, M. A. Robb, J. R. Cheeseman, G. Scalmani, V. Barone, G. A. Petersson, H. Nakatsuji, X. Li, M. Caricato, A. V. Marenich, J. Bloino, B. G. Janesko, R. Gomperts, B. Mennucci, H. P. Hratchian, J. V. Ortiz, A. F. Izmaylov, J. L. Sonnenberg, D. Williams-Young, F. Ding, F. Lipparini, F. Egidi, J. Goings, B. Peng, A. Petrone, T. Henderson, D. Ranasinghe, V. G. Zakrzewski, J. Gao, N. Rega, G. Zheng, W. Liang, M. Hada, M. Ehara, K. Toyota, R. Fukuda, J. Hasegawa, M. Ishida, T. Nakajima, Y. Honda, O. Kitao, H. Nakai, T. Vreven, K. Throssell, J. A. Montgomery, Jr, J. E. Peralta, F. Ogliaro, M. J. Bearpark, J. J. Heyd, E. N. Brothers, K. N. Kudin, V. N. Staroverov, T. A. Keith, R. Kobayashi, J. Normand, K. Raghavachari, A. P. Rendell, J. C. Burant, S. S. Iyengar, J. Tomasi, M. Cossi, J. M. Millam, M. Klene, C. Adamo, R. Cammi, J. W. Ochterski, R. L. Martin, K. Morokuma, O. Farkas, J. B. Foresman, and D. J. Fox, Gaussian, Inc, Wallingford CT, 2016.

[32] R. A. Kendall, T. H. Dunning Jr, R. J. Harrison, *J. Chem. Phys.* **1992**, *96*, 6796–6806.

[33] T. Yanai, D. P. Tew, N. C. Handy, *Chem. Phys. Lett.* **2004**, *393*, 51–57.

[34] E. Matito, *Phys. Chem. Chem. Phys.* **2016**, *18*, 11839–11846.

Manuscript received: July 21, 2023
Accepted manuscript online: September 24, 2023
Version of record online: October 6, 2023